SPANDIDOS PUBLICATIONS INTERNATIONAL JOURNAL OF MOLECULAR MEDICINE 42: 3083-3092, 2018

BML-111 suppresses TGF-β1-induced lung fibroblast activation *in vitro* and decreases experimental pulmonary fibrosis *in vivo*

YU-DONG JI[1*], ZHEN-LONG LUO[2*], CHUN-XIU CHEN[1], BO LI[1], JIE GONG[3], YA-XIN WANG[3], LIN CHEN[1], SHANG-LONG YAO[1] and YOU SHANG[3]

[1]Department of Anesthesiology, Institute of Anesthesiology and Critical Care, Union Hospital, Tongji Medical College, Huazhong University of Science and Technology; [2]Department of Gastroenterology, Tongji Hospital, Tongji Medical College, Huazhong University of Science and Technology; [3]Department of Critical Care Medicine, Institute of Anesthesiology and Critical Care, Union Hospital, Tongji Medical College, Huazhong University of Science and Technology, Wuhan, Hubei 430022, P.R. China

Received April 26, 2017; Accepted September 4, 2018

DOI: 10.3892/ijmm.2018.3914

Abstract. Pulmonary fibrosis is an aggressive end-stage disease. Transforming growth factor-β1 (TGF-β1) mediates lung fibroblast activation and is essential for the progress of pulmonary fibrosis. BML-111, a lipoxinA_4 (LXA_4) receptor (ALX) agonist, has been reported to possess anti-fibrotic properties. The present study aimed to elucidate whether BML-111 inhibits TGF-β1-induced mouse embryo lung fibroblast (NIH3T3 cell line) activation *in vitro* and bleomycin (BLM)-induced pulmonary fibrosis *in vivo*. *In vitro* experiments demonstrated that BML-111 treatment inhibits TGF-β1-induced NIH3T3 cell viability and the expression of smooth muscle α actin (α-SMA), fibronectin and total collagen. Furthermore, this suppressive effect was associated with mothers against decapentaplegic homolog (Smad)2/3, extracellular signal-regulated kinase (ERK) and Akt phosphorylation interference. *In vivo* experiments revealed that BML-111 treatment markedly improved survival rate and ameliorated the destruction of lung tissue structure. It also reduced interleukin-1β (IL-1β), tumor necrosis factor-α (TNF-α) and TGF-β1 expression in the BLM intratracheal mouse model. In addition, the expression ofα-SMA and extracellular matrix (ECM) deposition (total collagen, hydroxyproline and fibronectin) were also suppressed following BML-111 treatment. However, BOC-2, an antagonist of ALX, partially weakened the effects of BML-111. In conclusion, these results indicated that BML-111 inhibits TGF-β1-induced fibroblasts activation and alleviates BLM-induced pulmonary fibrosis. Therefore, BML-111 may be used as a potential therapeutic agent for pulmonary fibrosis treatment.

Correspondence to: Dr Shang-Long Yao, Department of Anesthesiology, Institute of Anesthesiology and Critical Care, Union Hospital, Tongji Medical College, Huazhong University of Science and Technology, 1277 Jiefang Avenue, Wuhan, Hubei 430022, P.R. China
E-mail: ysltian@163.com

Dr You Shang, Department of Critical Care Medicine, Institute of Anesthesiology and Critical Care, Union Hospital, Tongji Medical College, Huazhong University of Science and Technology, 1277 Jiefang Avenue, Wuhan, Hubei 430022, P.R. China
E-mail: you_shang@yahoo.com

[*]Contributed equally

Key words: pulmonary fibrosis, bleomycin, lipoxin, transforming growth factor-β1

Introduction

Pulmonary fibrosis is a common occurrence in the final stages of various lung diseases, including acute lung injury, drug reactions, sarcoidosis and autoimmune disease. Due to the lack of timely and effective intervention, the majority of patients who succumb to the disease exhibit respiratory failure 3-5 years following diagnosis (1). Therefore, identifying appropriate anti-fibrotic therapy is of vital importance (2-4).

Although the underlying mechanisms of pulmonary fibrosis are complex, previous studies have demonstrated that lung fibrosis develops from the maladaptive regulation of repair processes following lung injury and inflammation, where various profibrotic factors precipitate the formation of α smooth muscle actin (α-SMA)-expressing myofibroblasts, which in turn synthetize and secrete immoderate extracellular matrix (ECM) components, replacing normal lung tissue and driving lung fibrosis (5-7). It has been established that myofibroblasts originate from resident differentiated lung fibroblasts (8). The most important hallmark of fibroblast activation and differentiation is the expression of α-SMA (9). Transforming growth factor β1 (TGF-β1), a multifunctional molecule, is considered to be the most potent inducing mediator of fibroblast activation (10). TGF-β1 promotes fibroblast migration, proliferation and differentiation and promotes the production of ECM (11). The disruption of TGF-β1 mediated signaling inhibits fibroblast activation, thus preventing or improving pulmonary fibrotic response *in vivo* and *in vitro* (12).

Previous studies have revealed a strong association between inflammation, fibroblast activation and lung fibrosis (5-7). Infiltrating inflammatory cells within injured lung tissue release a high number of pro-fibrogenicmediators, which activate fibroblasts and induce lung fibrosis (13). Anti-inflammatory therapeutics are effective in extenuating pulmonary fibrosis (14). Lipoxins (LXs) are endogenous eicosanoids, which are generated either via 5- and 15-lipoxygenases, or via 5- and 12-lipoxygenases. They serve as the 'stop signal' for inflammation and exert potent anti-inflammatory and pro-resolution properties (15). LXA_4, as a principle LX, has been demonstrated to exert protective effects in various inflammation-associated diseases, including paracetamol-induced acute hepatic liver injury and lipopolysaccharide (LPS)-induced acute lung injury (16,17). In addition, LXA_4 serves primary roles in the regulation of tissue repair following inflammation, particularly in renal, skin and pulmonary fibrosis (18-20). In the dermal fibrosis model, LXA_4 is important for the inhibition of fibroblast proliferation and activation (19). LXA_4 acts through a specific G protein-coupled-receptor termed ALX to exert its multicellular effects. BML-111 is a lipoxinA_4 receptor (ALX) agonist and exerts its biological activity by binding to ALX (21). Previous studies have identified two different ALXs (ALX1/FPR-rs1 and ALX2/FPR2) in mice (22-25). BML-111 was initially considered to exert inhibitory effects similar to that of LXA_4 by inhibiting LTB4-induced neutrophil migration (26). Previous studies have demonstrated that BML-111 exhibits anti-inflammatory and pro-resolving effects in haemorrhagic shock-induced lung injury and ventilator-induced lung injury (27-29). Furthermore, a previous study revealed that BML-111 exerts protective effects on carbon tetrachloride (CCl_4)-induced hepatic fibrosis in rats (30). However, whether BML-111 affects fibroblast activation and lung fibrosis remains unknown.

In the present study, it was demonstrated that BML-111 reduces the expression of α-SMA, fibronectin and total collagen induced by TGF-β1 in NIH3T3 cells, and that it interferes with TGF-β1 associated signaling pathways. The results of the current study indicated that BML-111 inhibits the activation of fibroblasts and exerts direct anti-fibrotic affects. In addition, BML-111 treatment markedly improved murine survival rates in the BLM intratracheal mouse model, while BOC-2 (N-tert-butyloxy-carbonyl-phenyalanine-le-ucyl-phenyalanine-leucyl-phenyalanine) partially weakened the effects of BML-111. Furthermore, it was concluded that BML-111 alleviates BLM-induced pulmonary fibrosis by binding to ALX, and that these mechanisms may be involved in the anti-inflammatory response and in the inhibition of fibroblast activation.

Materials and methods

Cell culture. NIH3T3 cells were obtained from China Center for Type Culture Collection (Wuhan, China) and were cultured in Dulbecco's Modified Eagle's medium (DMEM; HyClone; GE Healthcare Life Sciences, Logan, UT, USA) to 75% confluence. The cells were then serum-starved for 12 h prior to each experiment. To select an optimal concentration of BML-111 (Cayman Chemical, Ann Arbor, MI, USA), cells were treated with varying concentrations (1, 10, 100, 200 and 500 nM) of BML-111 or vehicle (0.035% methanol) for 30 min at 37˚C prior to the addition of 5 ng/ml TGF-β1 (PeproTech Inc., Rocky Hill, NJ, USA) for 24 h at 37˚C. Although BML-111 at concentrations of 1 and 10 nM did not appear to affect a-SMA protein levels, the other concentrations of BML-111 substantially suppressed TGF-β1-induced a-SMA expression, with 200 and 500 nM concentrations producing the most notable effects. Notably, there was no substantial difference between these two concentrations. Therefore 200 nM BML-111 was selected for subsequent experiments. To assess whether the action of BML-111 is associated with ALX, 10 μM BOC-2 (Phoenix Pharmaceuticals, Inc., Burlingame, CA, USA) was supplemented to cells prior to BML-111 treatment for 30 min.

RNA isolation and reverse-transcriptase (RT) polymerase chain reaction (PCR). Total RNA was isolated from cultured cells using the TRIzol reagent (Invitrogen; Thermo Fisher Scientific Inc., Waltham, MA, USA). RNA reverse transcription was performed using an ReverTra Ace kit (Toyobo Life Science, Osaka, Japan). Briefly, the reaction was incubated in steps of 65˚C for 5 min, 37˚C for 15 min, 95˚C for 5 min and held at -20˚C. The amplified products of PCR were resolved using 2% agarose gel electrophoresis. The primers utilized were as follows: 5'-GGCAACTCTGTTGAGGAAAG-3' and 5'-GGCTCTCGGTAGACGAGA-3' for ALX homeobox 1 (ALX1)/formyl peptide receptor related sequence 1 (FPR-rs1); and 5'-GTCAA-GATCAACAGAAGAAACC-3' and 5'-GGG CTCTCTCAAGACTATAAGG-3' for ALX homeobox 2 (ALX2)/formyl peptide receptor 2 (FP-R2); and 5'-CTGAGA GGGAAATCGTGCGT-3' and 5'-CCACAGGATTCCATA CCCAAGA-3' for actin (25).

Immunofluorescence. For the detection of the expression of FPR2, NIH3T3 cells were cultured in DMEM at 37˚C for 24 h on sterile glass cover slips in 6-well plates and treated as aforementioned. Cells were then fixed with 4% paraformaldehyde. Following permeabilization, washing and blocking, the cells were incubated with rabbit anti-FPR2 antibodies (1:100; cat. no. AFR-002; Alomone Labs, Jerusalem, Israel) at 4˚C overnight and then washed and incubated with a fluorescent-labeled secondary antibody (fluorescein isothiocyanate-labelled goat anti-rabbit immunoglobulin G; 1:50; cat. no. AS1110; Aspen Biological, Wuhan, China) for 45 min at 37˚C. After washing again, over slips were mounted with anti-fade mounting medium (Beyotime Institute of Biotechnology, Haimen, China) on slides, and observed using a confocal microscope (Olympus FluoviewFV500).

Western blotting. Total protein was extracted using a Total Protein Extraction kit (Nanjing KeyGen Biotech Co., Ltd., Nanjing, China). The protein concentration was determined using a BCA Protein Assay kit (cat. no. KGP902; KeyGen Biotech Co., Ltd). A total of 30 μg protein from lung tissue or cells were separated on 8 or 10% SDS-PAGE, respectively and transferred onto a polyvinylidene difluoride membrane (Merck KGaA, Darmstadt, Germany). Membranes were blocked using 5% skimmed milk for 1 h at 4˚C. After incubating with primary antibodies overnight at 4˚C, the membrane was incubated with secondary antibodies [horseradish peroxidase (HRP) conjugated-Goat anti-Rabbit immunoglobulin G (IgG);

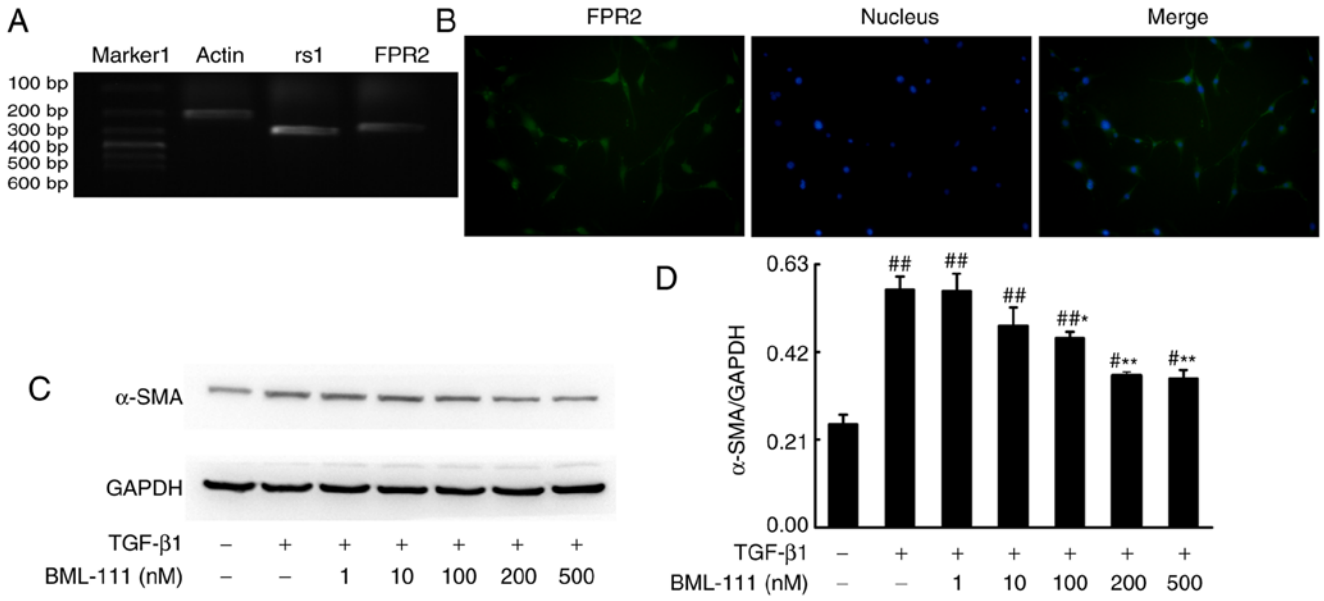

Figure 1. BML-111 decreased TGF-β1-induced NIH3T3 cell α-SMA expression in a dose-dependent manner. (A) NIH3T3 cells express rs1 and (B) FPR2. Cells were pretreated with a vehicle (0.035% ethanol) or BML-111 (1, 10, 100, 200 and 500 nM) for 30 min and then treated with TGF-β1 (5 ng/ml) for 24 h. (C) The expression of α-SMA was assessed using western blotting and (D) quantified. Similar results were obtained from at least 3 sections. Data are expressed as the mean ± standard deviation. #P<0.05 and ##P<0.01 vs. the vehicle group. *P<0.05 and **P<0.01 vs. the TGF-β1 group in the absence of BML-111. Magnification, x200. TGF-β1, Transforming growth factor-β1; α-SMA, smooth muscle α actin; rs1, related sequence 1; FPR2, formyl peptide receptor; marker 1, Trans DNA ladder (Tiangen Biotech, Co., Ltd., Beijing, China).

1:5,000; cat. no. ANT020 or HRP conjugated-Goat anti-Mouse IgG; 1:5,000; cat. no. ANT019] at room temperature for 1 h. Immunoreactive bands were detected using the Supersignal West Pico chemiluminescent substrate system (Pierce; Thermo Fisher Scientific Inc.) and analyzed using Quantity One Version 4.6.3 Image software (Bio-Rad Laboratories Inc., Hercules, CA, USA). The primary antibodies used were as follows: anti-fibronectin (1:1,000; cat. no. 1574-1), anti-α-SMA (1:1,000; cat. no. 1184-1), anti-pAkt (1:500; cat. no. 3188-1), anti-Akt (1:1,000; cat. no. 1085-1; each Epitomics; Abcam, Cambridge, UK); anti-mothers against decapentaplegic homolog (Smad)2/3 (1:500; cat. no. 5678), anti-phosphorylated (p) Smad2 (1:500; cat. no. 3108), anti-pSmad3 (1:500; cat. no. 9520), anti-p extracellular signal-regulated kinase (ERK; 1:500; cat. no. 4370), anti-ERK (1:1,000; cat. no. 4695; each Cell Signaling Technology Inc., Danvers, MA, USA) and anti-GAPDH (1:4,000; cat. no. LF-MA20175; Young In Frontier Co., Ltd., Seoul, Korea).

Collagen content determination. A total of 100 μl lung homogenates were extracted using 0.5 M acetic acid containing 0.6% pepsin and 200 μl NIH3T3 culture medium were mixed with 1 ml of Sircol dye reagent for 30 min at room temperature. Total collagen content was determined using the Sircol collagen assay kit (Biocolor Ltd., County Antrim, UK) according to manufacturer's protocol.

Cell viability assay. A total of 100 μl cells were seeded in 96-well plates (104 cells/ml), following serum starvation for 12 h. Cells were then pre-treated with or without BML-111 and BOC-2 for 30 min at 37˚C and cultured with or without TGF-β1 (5 ng/ml) for 24 h at 37˚C. Subsequently, MTT was added to the culture medium and cells were incubated for a further 4 h at 37˚C. The medium was then removed and 100 μl of dimethyl sulfoxide was added to each well and mixed for a further 10 min. The absorbance at 570 nm was determined using Sunrise™ (Tecan, Groedig, Austria).

Mice and grouping. C57BL/6 male mice (age, 6-8 weeks; weight, 20-25 g; n=76) were purchased from Beijing HFK Bioscience Co., Ltd. (Beijing, China) and housed in a specific pathogen-free animal facility. The mice were maintained under pathogen-free conditions, constant temperature, 22±2˚C; humidity, 40-50%; 12 h light/dark cycle and were given food and water *ad libitum*. The BLM-induced pulmonary fibrosis mouse model was established and validated according to a previously described method (31). Mice were randomly divided into 4 groups: A saline-injected group (sham group; n=10), a BLM-injected group treated with saline (untreated group; n=22), a BLM intratracheal injection group treated with BML-111 (BML-111 group; n=22), and a BOC-2 group (n=22). BOC-2 (Phoenix Pharmaceuticals, Inc., Burlingame, CA, USA) was injected to the BLM-injected mice treated with BML-111 before giving BML-111 30 min. Mortality was assessed daily until day 21 following BLM instillation. All surviving mice were then euthanized on the 21st day using an intraperitoneal injection of 200 mg/kg ketamine with 10 mg/kg xyalzine, followed by a thoracotomy (32-34). Lungs were removed during this procedure and at -80˚C for further analysis. Mice were sacrificed if the following humane endpoints were observed within the 21-day period: Body weight loss of >20%, impaired mobility, inability to retrieve food or water, labored breathing (increased respiratory rate and effort) and no response to external stimuli.

The use of mice within the present study was reviewed and approved by the Institutional Animal Care and Use Committee

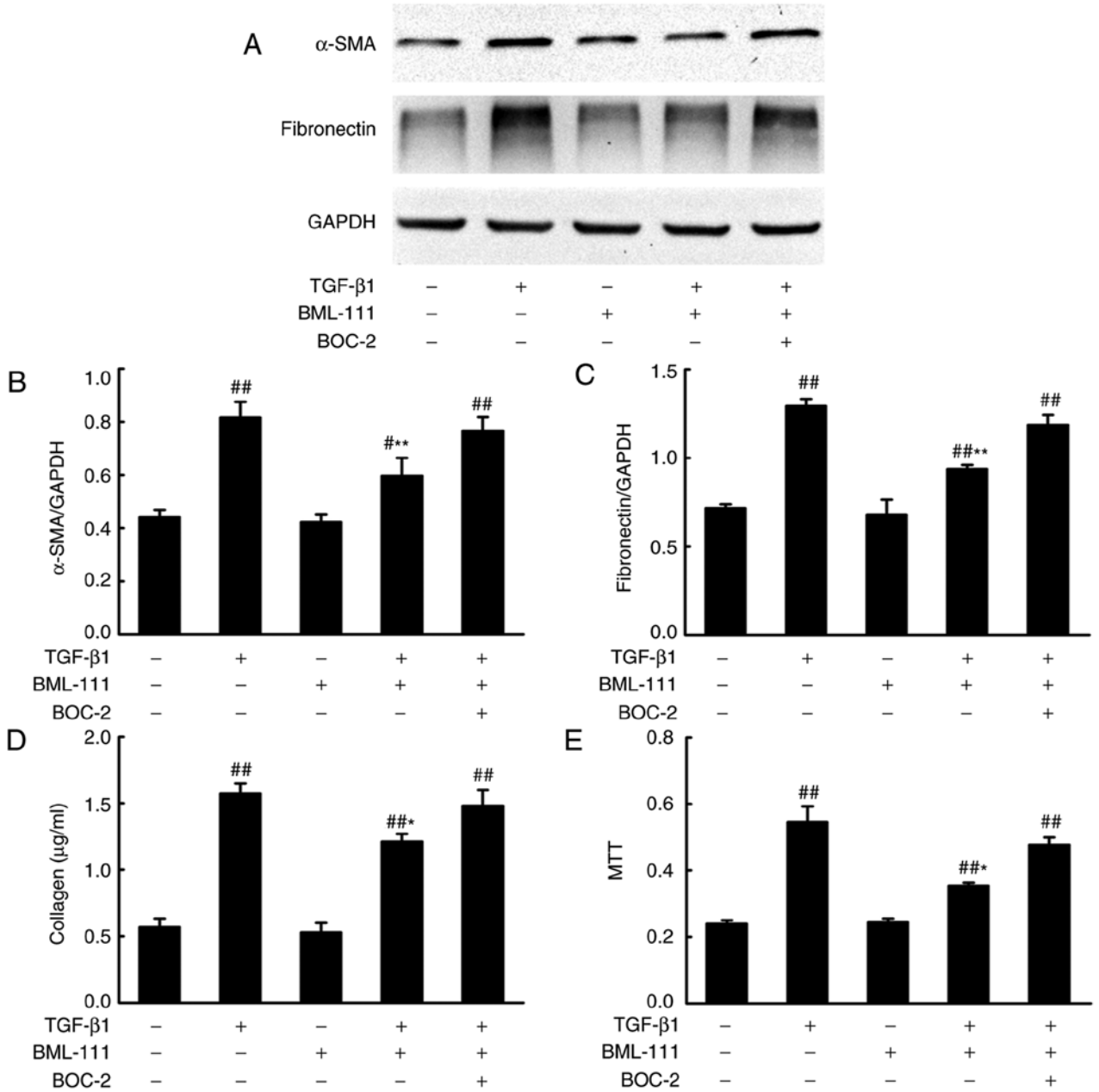

Figure 2. BML-111 suppressed TGF-β1-induced NIH3T3 cell activation. Cells were pretreated with a vehicle (0.035% ethanol) or BML-111 (200 nM) for 30 min in the absence or presence of BOC-2 (10 μM; administered 30 min prior to BML-111 treatment) and then stimulated with TGF-β1 (5 ng/ml) for 24 h. (A) The protein expression of α-SMA and fibronectin and the results of the western blot analysis quantified for (B) α-SMA and (C) fibronectin; and (D) total collagen concentration and (E) cell viability were assessed. Data are presented as the mean ± standard deviation for three independent experiments. $^{\#}$P<0.05 and $^{\#\#}$P<0.01 vs. the vehicle group. *P<0.05 and **P<0.01 vs. the TGF-β1 group in the absence of BML-111. TGF-β1, Transforming growth factor-β1; BOC-2, N-tert-butyloxy-carbonyl-phenyalanine-le-ucyl-phenyalanine-leucyl-phenyalanine; α-SMA, smooth muscle α actin.

of Tongji Medical College, Huazhong University of Science and Technology (Huazhong, China). All animal studies (including the mice euthanasia procedure) were completed in compliance with the regulations and guidelines of Huazhong University institutional animal care and conducted according to the AAALAC and the IACUC guidelines.

Histological analysis. Lung samples were fixed in 10% formalin for 24 h at room temperature, embedded in paraffin and sectioned onto slides at a thickness of 4-5 μm. Sections were stained with Masson's trichrome for detection of collagen deposition. For Masson's trichrome staining, tissue sections were stained with Weigert's hematoxylin stain for 10 min at room temperature and rinsed in lukewarm water for 5 min, immersed in acid ponceau/solferino for 15 min at room temperature, phosphomolybdic acid for 10 min at room temperature, and finally incubated with 2% aniline blue for 15 min at room temperature. The samples were also stained with hematoxylin and eosin (H&E) for 7 min and 15 sec respectively, at room temperature, for lung injury evaluation. Fibrosis scoring was evaluated according to Masson's trichrome and calculated as previously described by Ashcroft *et al* (35). The grade of lung fibrosis was scored as follows: 0, no pulmonary fibrosis; 1, mild pulmonary fibrosis, the affected area was <20%; 2, moderately

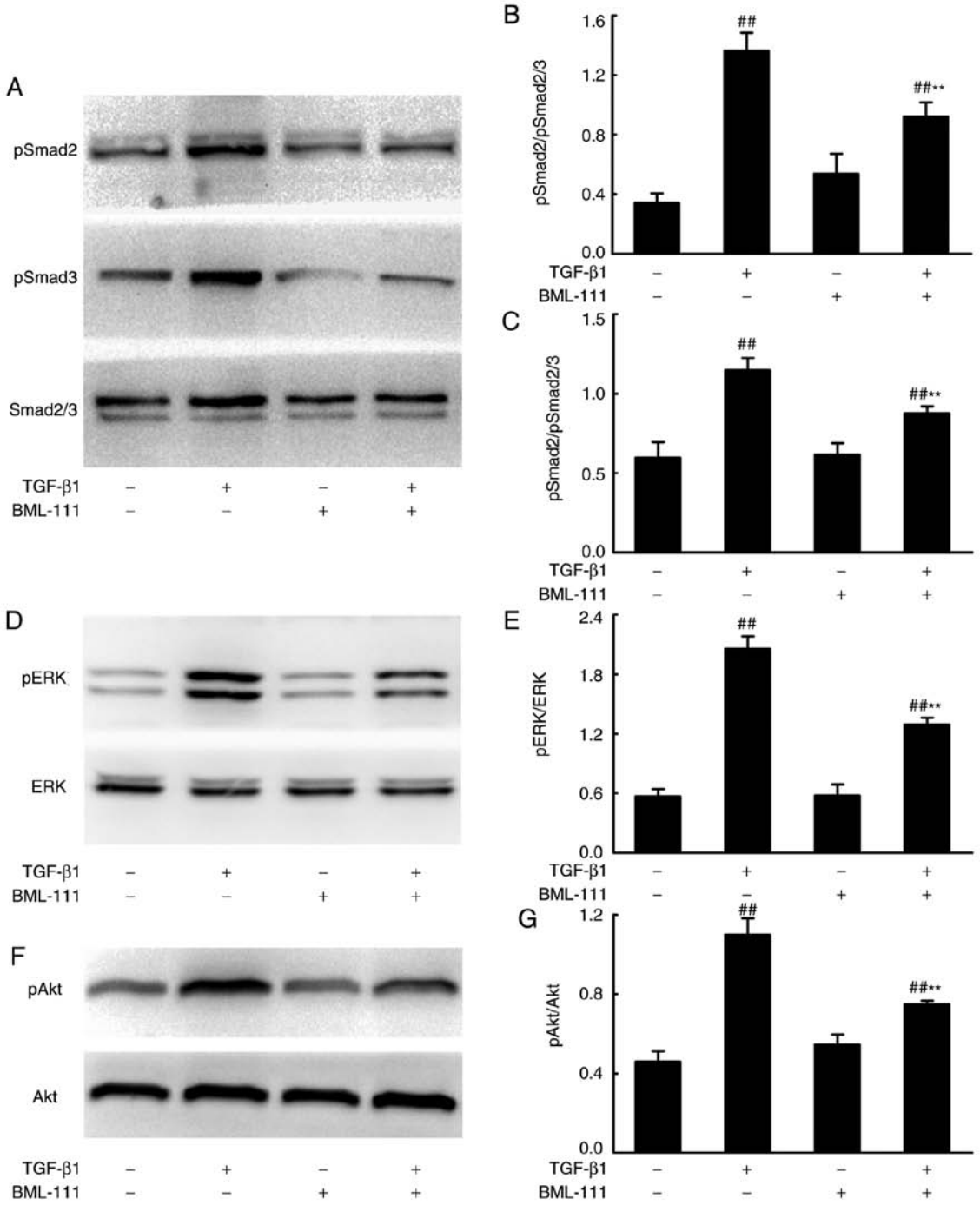

Figure 3. BML-111 inhibited TGF-β1-induced NIH3T3 cell Smad-dependent and Smad-independent signaling. NIH3T3 cells were stimulated using 5 ng/ml TGF-β1 in the absence or presence of 200 nM BML-111 (added 30 min prior to experimentation). Levels of (A) Smad2/3 and phosphorylated (B) Smad2/ (C) Smad3 were assessed. (D) ERK and (E) phosphorylated ERK, (F) Aktand (G) phosphorylated Aktwere also analyzed using western blotting, 24 h following cell stimulation. The figures are representative results of three independent experiments. Data are expressed as mean ± standard deviation. ##P<0.01 vs. the vehicle group. **P<0.01 vs. the TGF-β1 group in the absence of BML-111. TGF-β1, Transforming growth factor-β1; Smad2/3, mothers against decapentaplegic homolog 2/3; ERK, extracellular signal-regulated kinase.

pulmonary fibrosis, involvement of area of 20-50%; 3, severe pulmonary fibrosis, the affected area was >50%.

Hydroxyproline assay. Lung tissues were minced and hydrolyzed in 0.5 ml of 6 mol/l HCl for 6 h at 100˚C. After adjusting the pH to 6.0-6.8, activated carbon was added to hydrolyzation products (25 mg activated carbon with 4 ml diluted hydrolysate) diluted with distilled water. Samples were centrifuged at 1,445.5 x g for 10 min at room temperature and the supernatant was used to measure the hydroxyproline content with a Hydroxyproline assay kit (Nanjing Jiancheng Bioengineering Institute, Nanjing, China; cat. no. A030-3) according to the manufacturer's protocol.

ELISA for TGF-β1, IL-1β and TNF-α in bronchoalveolar lavage fluid (BALF). BALF was acquired according to a previously described method (36) and measured using ELISA kits (Wuhan Boster Biological Technology., Ltd., Wuhan, China) according the manufacturer's protocol.

Statistical analysis. Survival rates were evaluated using the log-rank (Mantel-Cox) test. Results were expressed as mean ± standard deviation and analyzed using one-way analysis of variance analysis followed by a Bonferoni post hoc test. Prism 5.0 (GraphPad Software, Inc., La Jolla, CA, USA) was used to perform statistical analysis. P<0.05 was considered to indicate a statistically significant result.

Results

BML-111 inhibits TGF-β1 induced NIH3T3 cell activation in vitro. BML-111 functions by binding to its corresponding receptor. As detected by PCR, NIH3T3 cells expressed rs1 and FPR2 (Fig. 1A and B). Activated lung fibroblasts, which express α-SMA and synthetize elevated ECM, serves a primary role in fibrogenesis. To determine whether BML-111 inhibits fibroblast activation, the effect of BML-111 on TGF-β1-induced NIH3T3 viability, α-SMA expression and the expression of various ECM components including the total collagen protein and fibronectin, was assessed. The results demonstrated that the stimulation of NIH3T3 cells with TGF-β1 significantly increases cell viability and the production of α-SMA, total collagen protein and fibronectin. NIH3T3 cell pretreatment with BML-111 markedly inhibits TGF-β1-induced NIH3T3 proliferation and the expression of α-SMA, total collagen protein and fibronectin. To further assess the role of the ALX in BML-111 activity, BOC-2 was added to the cells prior to treatment with BML-111. The results indicated that BOC-2 pretreatment inhibits the effect of BML-111 (Fig. 2).

BML-111 suppresses Smad-dependent and Smad-independent signaling pathways in TGF-β1-induced NIH3T3 cells. Smad-dependent and -independent signaling pathways mediate the pro-fibrotic effects of TGF-β1. To assess whether BML-111 mediated fibrosis is regulated by these pathways, the effect of BML-111 on TGF-β1-induced Smad2, Smad3, ERK and Akt phosphorylation in NIH3T3 cells were analyzed using western blotting. The results demonstrated that BML-111 significantly reduces pSmad2, pSmad3, pERK and pAkt levels in cells stimulated by TGF-β1 (Fig. 3).

BML-111 improves mice survival rate following BLM instillation. The survival rate of mice was monitored for 21 days following BLM injection. As presented in Fig. 4, no mice succumbed in the Sham group. BLM instillation without treatment led to a greater increased murine survival rate than the sham group, which primarily occurred between days 7 and 14. However, the majority of mice in the BML-111 group succumbed between day 11 and 18, pretreatment with BML-111 delayed and decreased mortality in mice with pulmonary fibrosis, and BOC-2 counteracted this effect of BML-111.

BML-111 decreases BLM-induced pulmonary fibrosis. BML-111 demonstrated a high efficiency in protecting lungs from fibrosis. As observed on H&E and Massion-stained slides (Fig. 5A-C), no pathological changes were observed in the lung tissue of the Sham group. Untreated, BOC-2 and BML-111 groups exhibited inflammatory cell infiltration, alveolar space collapse, alveolar wall thickening and extracellular collagen deposition. However the observed changes

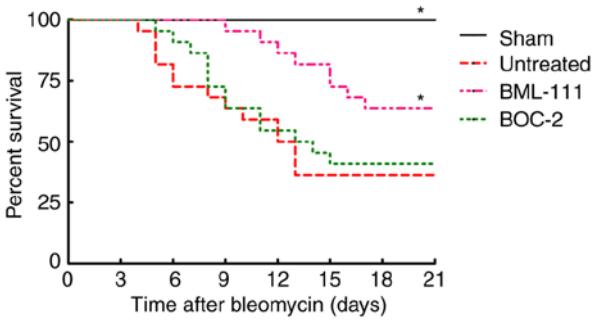

Figure 4. BML-111 treatment improved mortality after BLM instillation. Mice received intratracheal injection of 50 μl of saline (Sham group) or BLM 2 mg/kg (for untreated group, BML-111 group and BOC-2 group). Mice were treated intraperitoneally with the saline (for Sham group and untreated group) 1 ml or BML-111 (for BML-111 group and BOC-2 group) 1 mg/kg every other day from days 0 to 21, and BOC-2 group were given 50 μg/kg BOC-2 30 min before the addition of BML-111, and monitored daily for survival. Data are analyzed by Kaplan-Meier method (n=10 for the Sham group and n=22 for the others). *P<0.05 compared to the untreated group. BOC-2, N-tert-butyloxy-carbonyl-phenyalanine-le-ucyl-phenyalanine-leucyl-phenyalanine.

were less severe in the BML-111 group. The lung tissues of BLM-treated mice exhibited significantly upregulated levels of ECM and α-SMA, which is typical of fibrosis. However, these levels were significantly suppressed following BML-111 treatment (Fig. 6). In addition, the BLM injection administered to the untreated group significantly upregulated the production of TGF-β1, TNF-α and IL-1β in BALF compared with the Sham group. The BML-111 group exhibited a reduction in these cytokines compared with the BLM and BOC-2 group, and BOC-2 counteracted the effect of BML-111 (Fig. 5D-F).

Discussion

Lung fibrosis can be divided into two stages: The inflammatory and fibrotic stage. During the inflammatory stage, inflammatory cells infiltrate into the area of injury, attempt to clear tissue debris, and replace damaged cells (7). In the fibrotic phase, activated cytokines, including TGF-β1, induce the formation of myofibroblasts, which synthesize excessive ECM components and thus precipitate tissue remodeling (11). Previously, it has been demonstrated that BML-111 effectively mitigates the inflammatory response following lung injury (21). However, studies have assessed its direct anti-fibrotic actions. The present study demonstrated that BML-111 treatment inhibited TGF-β1 mediated NIH3T3 proliferation and activation as well as the synthesis and expression of ECM components. Furthermore, it was also revealed that BML-111 attenuated fibrotic changes following BLM instillation in mice and that thisprotective effect was partially counteracted following BOC-2 pretreatment.

BML-111 is a commercially stable ALX agonist, which possesses excellent anti-inflammatory and pro-resolving action, similar to that of LXA_4. BML-111 suppresses pulmonary inflammatory reactions in ventilator/hemorrhagic shock/LPS-induced lung injury (27,29,37). Previously, it has been demonstrated that human lung fibroblasts in fibrotic lung tissue express ALX and that LXA_4 decreases TGF-β1 and connective tissue growth factor dependent profibrotic activity in human lung myofibroblasts (38,39). Although it has been

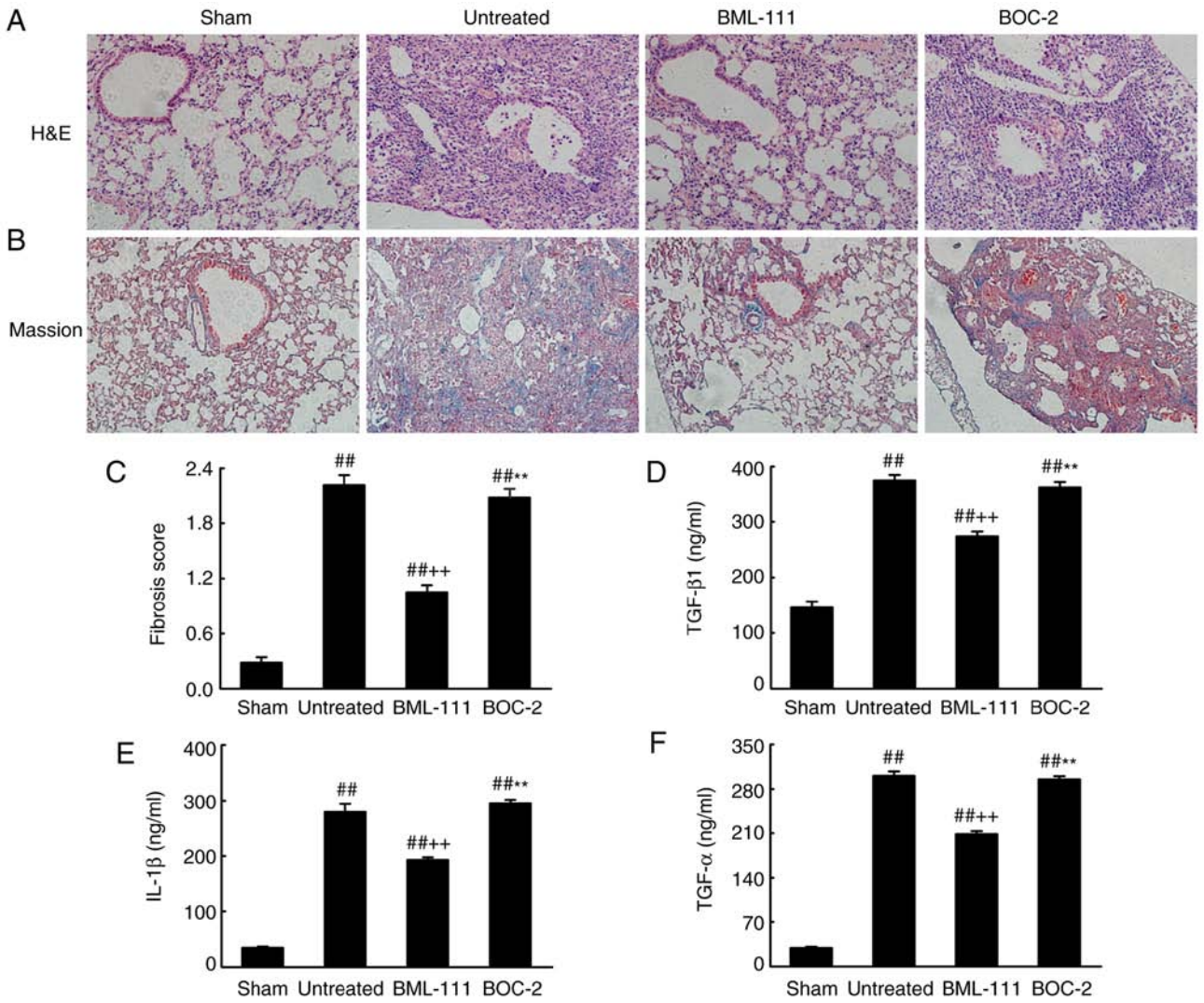

Figure 5. BML-111 treatment mitigated the destruction of lung architecture and production of TGF-β1, TNF-α and IL-1β in BALF following BLM iniection. Mice were treated with 50 μl saline (Sham group) or 2 mg/kg BLM (untreated group, BML-111 group and BOC-2 group) at day 0 were intraperitoneally administered with 1 ml of saline (Sham group and untreated group) or 1 mg/kg of BML-111 (BML-111 group and BOC-2 group) in the presence or absence of 50 μg/kg BOC-2 (BOC-2 group) prior to the administration of BML-111. Mice were then sacrificed on day 21 and the extent of pulmonary injury and fibrosis were assessed using (A) H&E and (B) Masson's trichrome staining (magnification, x100). (C) Fibrotic score was measured using the Ashcroft method. Levels of (D) TGF-β1, (E) TNF-α and (F) IL-1β in BALF were determined using ELISA. Data are expressed as mean ± standard deviation (n=8). $^{\#\#}$P<0.01 vs. the Sham group. $^{++}$P<0.01 vs. the untreated group. **P<0.01 vs. the BML-111 group. TGF-β1, Transforming growth factor-β1; TNF-α, tumor necrosis factor α; IL-1β, interleukin 1β; BALF, bronchoalveolar lavage fluid; BLM, bleomycin; BOC-2, N-tert-butyloxy-carbonyl-phenyalanine-le-ucyl-phenyalanine-leucyl-phenyalanine.

revealed that BML-111 inhibitsCCl_4-induced hepatic fibrosis *in vivo*, no assessment has been made on its effect on fibroblast activation *in vitro* (30). The present study detected the expression of ALX in NIH3T3 cells and demonstrated that BML-111 treatment inhibited TGF-β1 triggered increases of α-SMA in a dose-dependent manner, with a maximum effect at 200 nM. Furthermore, 200 nM BML-111 treatment mitigated TGF-β1-induced cell proliferation and the production of ECM, including total collagen and fibronectin. This indicated that BML-111 treatment inhibits fibroblast activation and exerts a direct anti-fibrosis effect *in vitro*. However, the activity of BML-111 is abrogated by BOC-2, which indicates that this effect is receptor dependent.

TGF-β1 mediated fibroblast activation occurs primarily via Smad-dependent and independent pathways. To further investigate the mechanisms by which BML-111 inhibits TGF-β1-mediated NIH3T3 cell activation, the downstream components of TGF-β1 signaling were determined. The results indicated that BML-111 inhibits TGF-β1-induced phosphorylation of Smad2 and Smad3. Previous studies have also demonstrated that phosphorylated Smad2 and Smad3 integrate with Smad4 and translocate into the nucleus from the cytoplasm, where they ultimately activate the transcription of pro-fibrotic genes, including collagen I, fibronectin and α-SMA through reaction cascades (40,41). The current study demonstrated that BML-111 treatment inhibits the phosphorylation of non-Smad-dependent pathways including ERK and Akt. Previous studies have revealed that phosphorylated ERK and Akt are involved in TGF-β1 induced ECM increase, while ERK is involved in fibroblast proliferation (42-44). Thus, these results indicate that BML-111 acts as an anti-fibrotic agent by inhibiting the TGF-β1 associated signaling pathway.

BLM is widely used to induce pulmonary fibrosis in mice. Following BLM instillation, mice are infected with acute

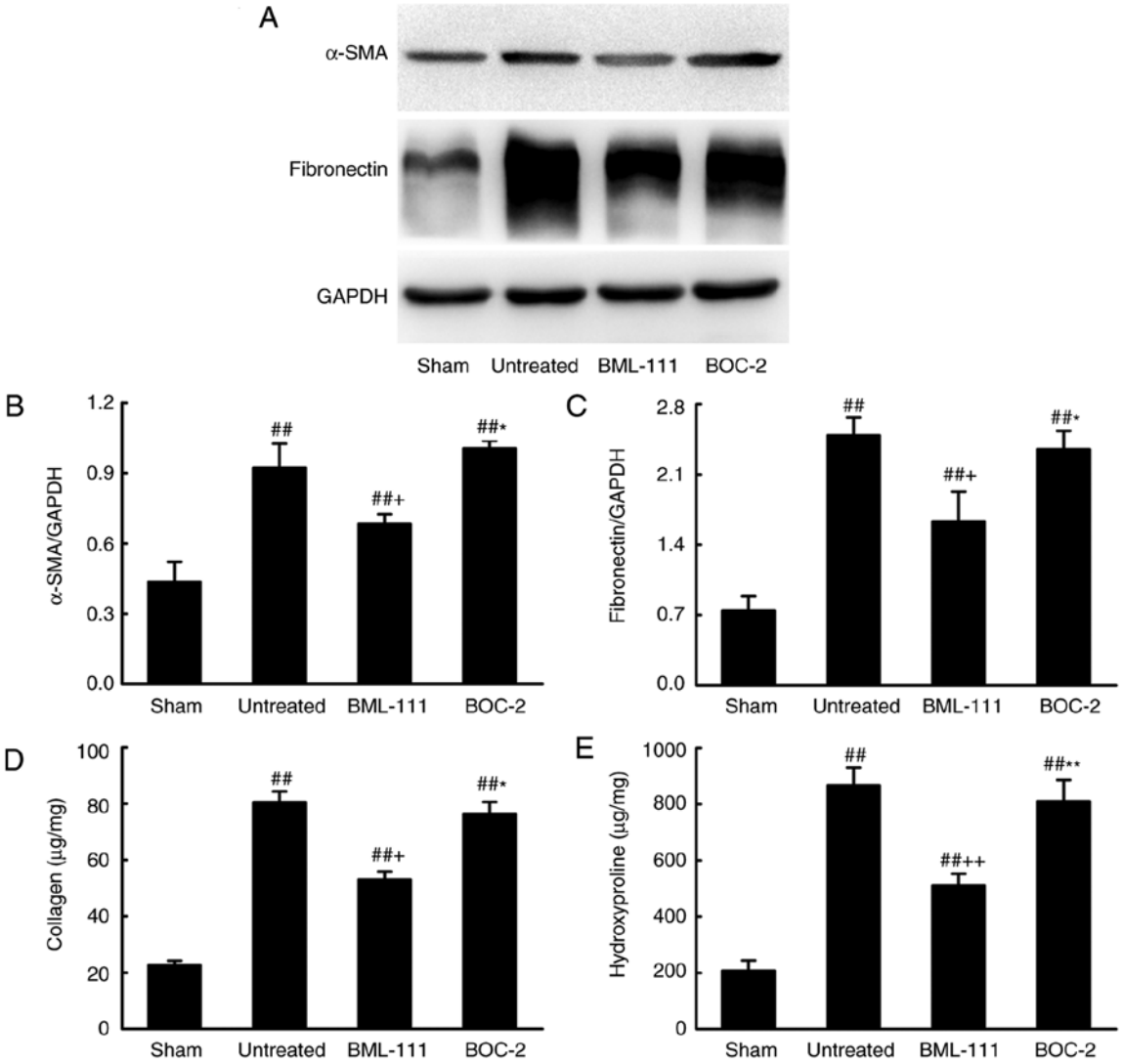

Figure 6. BML-111 treatment inhibited α-SMA expression and ECM deposition in lungs following BLM injection. Mice treated with 50 μl saline (Sham group) or 2 mg/kg BLM (untreated group, BML-111 group and BOC-2 group) at day 0 were intraperitoneally injected with 1 ml saline (Sham and untreated group) or 1 mg/kg of BML-111 (BML-111 group and BOC-2 group) with or without 50 μg/kg BOC-2 (BOC-2 group) every other day from day 0-21. Mice were sacrificed on day 21 and the expression of (A and B) α-SMA and (C) fibronectin was detected using western blotting. (D) Total collagen protein was measured using a Sircol collagen assay kit, and the content of (E) hydroxyproline was determined using a Hydroxyproline assay kit. Data are expressed as mean ± standard deviation. $^{\#\#}$P<0.01 vs. the Sham group. $^{+}$P<0.05 and $^{++}$P<0.01 vs. the untreated group. *P<0.05, **P<0.01 vs. the BML-111 group. α-SMA, smooth muscle α actin; ECM, extracellular matrix; BLM, bleomycin.

alveolitis within 2-3 days, where upon pro-fibrosis media is released, initiating ECM synthesis and the progression to fibrosis (45). The anti-fibrotic effects of BML-111 were examined using this model in the current study (45). The results indicated that BML-111 treatment markedly reduced the destruction of lung tissue and structure. In addition, BML-111 inhibited BLM-induced expression of α-SMA and ECM accumulation. These results were consistent with *in vitro* results. Furthermore, it was revealed that IL-1β, TNF-α and TGF-β1 in BALF was also decreased following BML-111 administration. IL-1β and TNF-α are vital pro-inflammatory cytokines that cause the further release of fibrosis media and perpetuate the fibrotic cascade (13). Additionally, TGF-β1 also counteracts fibroblast apoptosis and attenuates ECM degradation (46-48). The results of the present study also demonstrated that BML-111 administration delayed and decreased the mortality of mice. This confirmed that BML-111 exerts a protective effect on lung fibrosis, which may be attributed to anti-inflammatory action, the down-regulation of TGF-β1 expression and the inhibition of fibroblasts activation. Similarly, this effect is receptor dependent.

To conclude, the present study demonstrated that BML-111 treatment suppresses TGF-β1-induced fibroblast α-SMA protein synthesis and total collagen and fibronectin expression, by suppressing Smad-dependent and Smad-independent signaling pathways. Furthermore, BML-111 inhibited TGF-β1 levels and the synthesis of inflammatory mediators in BLM-induced pulmonary fibrosis. These results indicate that BML-111 may be used as a potential agent for the treatment of pulmonary fibrosis.

Acknowledgements

Not applicable.

Funding

The present study was supported by grants obtained from the National Natural Science Foundation of China (grant nos. 30930089, 81372036, 81671890, 81500064, 81601669 and 81500436) and the Key Clinical Project of Ministry of Health of China (grant. No. 2010-47).

Availability of data and materials

The analyzed data sets generated during the present study are available from the corresponding author on reasonable request.

Authors' contributions

YDJ, SLY and YS produced substantial contributions to the conception and design of the present study. YDJ, ZLL, CXC, BL and JG performed the experiments. ZLL, YXW and LC analyzed the data. YDJ and ZLL drafted the paper. YS edited and revised the manuscript. All authors read and approved the final manuscript.

Ethics approval and consent to participate

The use of mice within the present study was reviewed and approved by the Institutional Animal Care and Use Committee of Tongji Medical College, Huazhong University of Science and Technology (Huazhong, China).

Patient consent for publication

Not applicable.

Competing interests

The authors declare that they have no competing interests.

References

1. King TJ Jr, Tooze JA, Schwarz MI, Brown KR and Cherniack RM: Predicting survival in idiopathic pulmonary fibrosis: Scoring system and survival model. Am J Respir Crit Care Med 164: 1171-1181, 2001.
2. Dempsey OJ: Clinical review: Idiopathic pulmonary fibrosis-past, present and future. Respir Med 100: 1871-1885, 2006.
3. Noble PW, Barkauskas CE and Jiang D: Pulmonary fibrosis: Patterns and perpetrators. J Clin Invest 122: 2756-2762, 2012.
4. du Bois RM: Strategies for treating idiopathic pulmonary fibrosis. Nat Rev Drug Discov 9: 129-140, 2010.
5. Wynn TA: Cellular and molecular mechanisms of fibrosis. J Pathol 214: 199-210, 2008.
6. Wynn TA: Integrating mechanisms of pulmonary fibrosis. J Exp Med 208: 1339-1350, 2011.
7. Todd NW, Luzina IG and Atamas SP: Molecular and cellular mechanisms of pulmonary fibrosis. Fibrogenesis Tissue Repair 5: 11, 2012.
8. Phan SH: Biology of fibroblasts and myofibroblasts. Proc Am Thorac Soc 5: 334-337, 2008.
9. Cutroneo KR, White SL, Phan SH and Ehrlich HP: Therapies for bleomycin induced lung fibrosis through regulation of TGF-beta1 induced collagen gene expression. J Cell Physiol 211: 585-589, 2007.
10. Sivakumar P, Ntolios P, Jenkins G and Laurent G: Into the matrix: Targeting fibroblasts in pulmonary fibrosis. Curr Opin Pulm Med 18: 462-469, 2012.
11. Lee CG, Cho S, Homer RJ and Elias JA: Genetic control of transforming growth factor-beta1-induced emphysema and fibrosis in the murine lung. Proc Am Thorac Soc 3: 476-477, 2006.
12. Caraci F, Gili E, Calafiore M, Failla M, La Rosa C, Crimi N, Sortino MA, Nicoletti F, Copani A and Vancheri C: TGF-beta1 targets the GSK-3beta/beta-catenin pathway via ERK activation in the transition of human lung fibroblasts into myofibroblasts. Pharmacol Res 57: 274-282, 2008.
13. Wynn TA and Ramalingam TR: Mechanisms of fibrosis: Therapeutic translation for fibrotic disease. Nat Med 18: 1028-1040, 2012.
14. Pourgholamhossein F, Rasooli R, Pournamdari M, Pourgholi L, Samareh-Fekri M, Ghazi-Khansari M, Iranpour M, Poursalehi HR, Heidari MR and Mandegary A: Pirfenidone protects against paraquat-induced lung injury and fibrosis in mice by modulation of inflammation, oxidative stress, and gene expression. Food Chem Toxicol 112: 39-46, 2018.
15. Romano M, Cianci E, Simiele F and Recchiuti A: Lipoxins and aspirin-triggered lipoxins in resolution of inflammation. Eur J Pharmacol 760: 49-63, 2015.
16. Xia J, Zhou XL, Zhao Y, Zhu YQ, Jiang S and Ni SZ: Roles of lipoxin A4 in preventing paracetamol-induced acute hepatic injury in a rabbit model. Inflammation 36: 1431-1439, 2013.
17. Jiang X, Li Z, Jiang S, Tong X, Zou X, Wang W, Zhang Z, Wu L and Tian D: Lipoxin A4 exerts protective effects against experimental acute liver failure by inhibiting the NF-κB pathway. Int J Mol Med 37: 773-780, 2016.
18. Börgeson E, Docherty NG, Murphy M, Rodgers K, Ryan A, O'Sullivan TP, Guiry PJ, Goldschmeding R, Higgins DF and Godson C: Lipoxin A_4 and benzo-lipoxin A_4 attenuate experimental renal fibrosis. FASEB J 25: 2967-2979, 2011.
19. Krönke G, Reich N, Scholtysek C, Akhmetshina A, Uderhardt S, Zerr P, Palumbo K, Lang V, Dees C, Distler O, *et al*: The 12/15-lipoxygenase pathway counteracts fibroblast activation and experimental fibrosis. Ann Rheum Dis 71: 1081-1087, 2012.
20. Martins V, Valença SS, Farias-Filho FA, Molinaro R, Simões RL, Ferreira TP, e Silva PM, Hogaboam CM, Kunkel SL, Fierro IM, *et al*: ATLa, an aspirin-triggered lipoxin A4 synthetic analog, prevents the inflammatory and fibrotic effects of bleomycin-induced pulmonary fibrosis. J Immunol 182: 5374-5381, 2009.
21. Gong J, Guo S, Li HB, Yuan SY, Shang Y and Yao SL: BML-111, a lipoxin receptor agonist, protects haemorrhagic shock-induced acute lung injury in rats. Resuscitation 83: 907-912, 2012.
22. Fiore S, Maddox JF, Perez HD and Serhan CN: Identification of a human cDNA encoding a functional high affinity lipoxin A4 receptor. J Exp Med 180: 253-260, 1994.
23. Takano T, Fiore S, Maddox JF, Brady HR, Petasis NA and Serhan CN: Aspirin-triggered 15-epi-lipoxin A4 (LXA4) and LXA4 stable analogues are potent inhibitors of acute inflammation: Evidence for anti-inflammatory receptors. J Exp Med 185: 1693-1704, 1997.
24. Gao JL, Chen H, Filie JD, Kozak CA and Murphy PM: Differential expansion of the N-formylpeptide receptor gene cluster in human and mouse. Genomics 51: 270-276, 1998.
25. Wang YP, Wu Y, Li LY, Zheng J, Liu RG, Zhou JP, Yuan SY, Shang Y and Yao SL: Aspirin-triggered lipoxin A4 attenuates LPS-induced pro-inflammatory responses by inhibiting activation of NF-κB and MAPKs in BV-2 microglial cells. J Neuroinflammation 8: 95, 2011.
26. Lee TH, Lympany P, Crea AE and Spur BW: Inhibition of leukotriene B4-induced neutrophil migration by lipoxin A4: structure-function relationships. Biochem Biophys Res Commun 180: 1416-1421, 1991.
27. Li HB, Wang GZ, Gong J, Wu ZY, Guo S, Li B, Liu M, Ji YD, Tang M, Yuan SY, *et al*: BML-111 attenuates hemorrhagic shock-induced acute lung injury through inhibiting activation of mitogen-activated protein kinase pathway in rats. J Surg Res 183: 710-719, 2013.
28. Gong J, Li HB, Guo S, Shang Y and Yao SL: Lipoxin receptor agonist, may be a potential treatment for hemorrhagic shock-induced acute lung injury. Med Hypotheses 79: 92-94, 2012.
29. Li H, Wu Z, Feng D, Gong J, Yao C, Wang Y, Yuan S, Yao S and Shang Y: BML-111, a lipoxin receptor agonist, attenuates ventilator-induced lung injury in rats. Shock 41: 311-316, 2014.
30. Zhou XY, Yu ZJ, Yan D, Wang HM, Huang YH, Sha J, Xu FY, Cai ZY and Min WP: BML-11, a lipoxin receptor agonist, protected carbon tetrachloride-induced hepatic fibrosis in rats. Inflammation 36: 1101-1106, 2013.
31. Izumo T, Kondo M and Nagai A: Effects of a leukotriene B4 receptor antagonist on bleomycin-induced pulmonary fibrosis. Eur Respir J 34: 1444-1451, 2009.

32. Kelly MN, Zheng M, Ruan S, Kolls J, D'Souza A and Shellito JE: Memory $CD4^+$ T cells are required for optimal NK cell effector functions against the opportunistic fungal pathogen Pneumocystis murina. J Immunol 190: 285-295, 2013.
33. Yang J, Nan C, Ripps H and Shen W: Destructive changes in the neuronal structure of the FVB/N mouse retina. PLoS One 10: e129719, 2015.
34. AVMA Guodelines for the Euthanasia of Animals: 2013 Edition. p48.
35. Ashcroft T, Simpson JM and Timbrell V: Simple method of estimating severity of pulmonary fibrosis on a numerical scale. J Clin Pathol 41: 467-470, 1988.
36. Liu J, Wei Y, Luo Q, Xu F, Zhao Z, Zhang H, Lu L, Sun J, Liu F, Du X, *et al*: Baicalin attenuates inflammation in mice with OVA-induced asthma by inhibiting NF-κB and suppressing CCR7/CCL19/CCL21. Int J Mol Med 38: 1541-1548, 2016.
37. Tang M, Chen L, Li B, Wang Y, Li S, Wen A, Yao S and Shang Y: BML-111 attenuates acute lung injury in endotoxemic mice. J Surg Res 200: 619-630, 2016.
38. Roach KM, Feghali-Bostwick CA, Amrani Y and Bradding P: Lipoxin A4 Attenuates constitutive and TGF-β1-dependent profibrotic activity in human lung myofibroblasts. J Immunol 195: 2852-2860, 2015.
39. Wu SH, Wu XH, Lu C, Dong L and Chen ZQ: Lipoxin A4 inhibits proliferation of human lung fibroblasts induced by connective tissue growth factor. Am J Respir Cell Mol Biol 34: 65-72, 2006.
40. Mendoza JA, Jacob Y, Cassonnet P and Favre M: Human papillomavirus type 5 E6 oncoprotein represses the transforming growth factor beta signaling pathway by binding to SMAD3. J Virol 80: 12420-12424, 2006.
41. Hasegawa M, Matsushita Y, Horikawa M, Higashi K, Tomigahara Y, Kaneko H, Shirasaki F, Fujimoto M, Takehara K and Sato S: A novel inhibitor of Smad-dependent transcriptional activation suppresses tissue fibrosis in mouse models of systemic sclerosis. Arthritis Rheum 60: 3465-3475, 2009.
42. Runyan CE, Schnaper HW and Poncelet AC: The phosphatidylinositol 3-kinase/Akt pathway enhances Smad3-stimulated mesangial cell collagen I expression in response to transforming growth factor-beta1. J Biol Chem 279: 2632-2639, 2004.
43. Xiao L, Du Y, Shen Y, He Y, Zhao H and Li Z: TGF-beta 1 induced fibroblast proliferation is mediated by the FGF-2/ERK pathway. Front Biosci (Landmark Ed) 17: 2667-2674, 2012.
44. Hinz B: Myofibroblasts. Exp Eye Res 142: 56-70, 2016.
45. Mouratis MA and Aidinis V: Modeling pulmonary fibrosis with bleomycin. Curr Opin Pulm Med 17: 355-361, 2011.
46. Kolb M, Margetts PJ, Anthony DC, Pitossi F and Gauldie J: Transient expression of IL-1beta induces acute lung injury and chronic repair leading to pulmonary fibrosis. J Clin Invest 107: 1529-1536, 2001.
47. Sime PJ, Marr RA, Gauldie D, Xing Z, Hewlett BR, Graham FL and Gauldie J: Transfer of tumor necrosis factor-alpha to rat lung induces severe pulmonary inflammation and patchy interstitial fibrogenesis with induction of transforming growth factor-beta1 and myofibroblasts. Am J Pathol 153: 825-832, 1998.
48. Sheppard D: Transforming growth factor beta: A central modulator of pulmonary and airway inflammation and fibrosis. Proc Am Thorac Soc 3: 413-417, 2006.

This work is licensed under a Creative Commons Attribution-NonCommercial-NoDerivatives 4.0 International (CC BY-NC-ND 4.0) License.